

## Supporting Information

### Cycloaddition Reactivity of Yb@ $D_{3h}$ -C<sub>74</sub>: the Carbon Cage Size

#### Matters

Muqing Chen <sup>‡,\*a,b</sup>, Wenhao Xiang <sup>‡,b</sup>, Xinde Li <sup>c</sup>, Jinpeng Xin <sup>b</sup>, Peng Jin <sup>\*c</sup>,  
Yongfu Qiu<sup>a</sup>, Zhiyu Chen <sup>a</sup>, Shangfeng Yang <sup>\*b</sup>

<sup>a</sup> School of Materials Science and Engineering, Research Institute of Interdisciplinary Science (RISE), Dongguan University of Technology, Guangdong 523808, China, E-mail: mqchen@ustc.edu.cn;

<sup>b</sup> State Key Laboratory of Precision and Intelligent Chemistry, Collaborative Innovation Center of Chemistry for Energy Materials (iChEM), School of Chemistry and Materials Science, University of Science and Technology of China, Hefei 230026, China. E-mail: sfyang@ustc.edu.cn.

<sup>c</sup> School of Materials Science and Engineering, Hebei University of Technology, Tianjin 300130, China. E-mail: china.peng.jin@gmail.com;

‡ These authors contributed equally to this work.

#### Contents:

1. Computational details.....	S2
2. HPLC purification and MALDI-TOF MS characterization of Yb@ $D_{3h}$ -C <sub>74</sub> ....	S3
3. HPLC purification and MALDI-TOF MS characterization of <b>2a-2c</b> .....	S3
4. Metal atom disorders and the relative position of major Yb site and center of carbon cage in Yb@ $D_{3h}$ -C <sub>74</sub> and <b>2a</b> .....	S4
5. Crystal data of Yb@ $D_{3h}$ -C <sub>74</sub> and <b>2a</b> .....	S4
6. Theoretical calculation of Yb@ $D_{3h}$ -C <sub>74</sub> and <b>2a</b> .....	S5
7. Electrochemical data of Yb@ $D_{3h}$ -C <sub>74</sub> and	

**2a.....S7**

## 1. Computational Method:

Geometry optimizations were conducted by using the PBE0 functional<sup>[1]</sup> in conjunction with the standard 6-31G\* all-electron basis set for the H, C, N and Cl atoms<sup>[2]</sup>, and the Stuttgart/Dresden quasi-relativistic effective core potential (ECP) and corresponding basis set (SDD) for the Yb atom.<sup>[3]</sup> Such a level of theory is denoted here as PBE0/6-31G\*~SDD for simplicity. All the DFT calculations were carried out by using the Gaussian 16 software package.<sup>[4]</sup> The Mercury<sup>[5]</sup> program was employed to visualize the results.

## 2. Separation, purification and mass spectrum of Yb@D<sub>3h</sub>-C<sub>74</sub>.

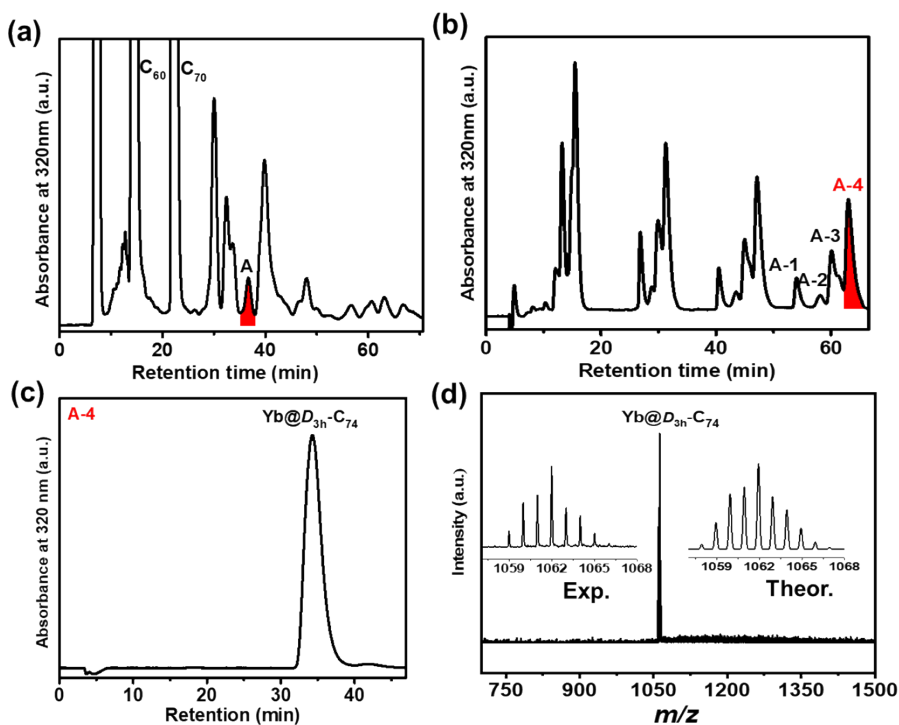


**Figure. S1** (a) The HPLC profiles of the raw solution extracted from the carbon soot. Conditions: BP column (20 mm×250 mm); flow rate 10.0 mL min<sup>-1</sup>; injection volume 10.0 mL; toluene as the eluent. (b) The HPLC profile of the toluene solution containing Yb@D<sub>3h</sub>-C<sub>74</sub> in second-step separation. Conditions: BPM column (20 mm×250 mm); flow rate 15.0 mL min<sup>-1</sup>; injection volume 5.0 mL; toluene as the eluent. (c) The HPLC profile of the toluene solution containing Yb@D<sub>3h</sub>-C<sub>74</sub> in third-step separation. Conditions: 5PBB column (10 mm×250 mm); flow rate 5.0 mL min<sup>-1</sup>; injection volume 5.0 mL; toluene as the eluent. (d) MALDI-TOF mass spectrum of Yb@D<sub>3h</sub>-C<sub>74</sub> collected by three-step HPLC purification.

### 3. The HPLC purification and MALDI-TOF MS characterization of **2a**-**2c**.

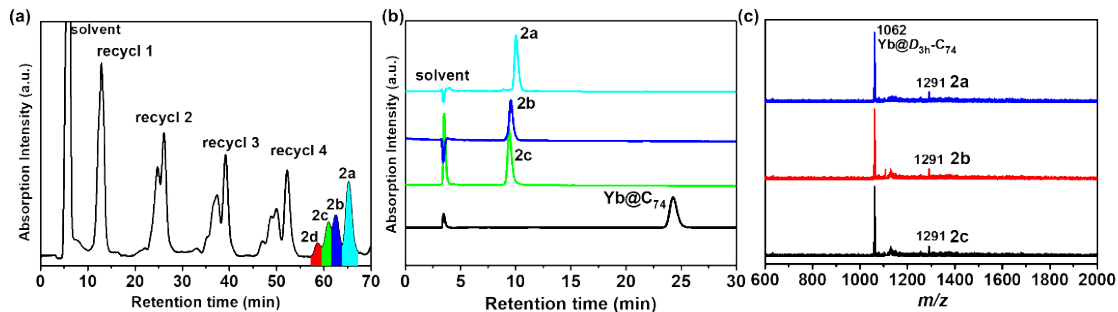


**Figure. S2** (a) The prepared HPLC profiles of  $\text{Yb}@\text{D}_{3h}\text{-C}_{74}$  derivatives using a BP column (10 mm×250 mm); flow rate 5.0 mL min<sup>-1</sup>; injection volume 5 mL; toluene as the eluent. (b) The analytical HPLC profile of pure isomeric adducts **2a**, **2b**, **2c**. Conditions: BP column (2.5 mm×250 mm); flow rate 1.0 mL min<sup>-1</sup>; injection volume 20  $\mu$ L; toluene as the eluent. (c) MALDI-TOF mass spectrum of pure isomeric adducts **2a**, **2b**, **2c**.

### 4. Metal atom disorders and the relative position of major Yb site and center of carbon cage in $\text{Yb}@\text{D}_{3h}\text{-C}_{74}$ and **2a**

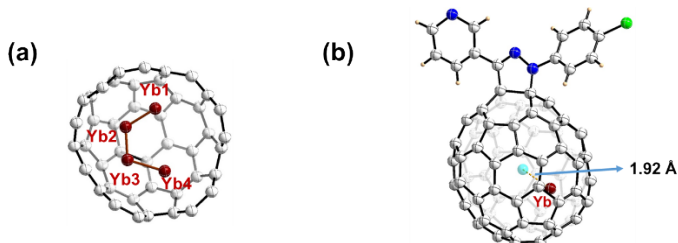


**Figure S3.** The position disorders of the encapsulated Yb ion in (a) **2a**, the grafted moiety was omitted for clarity; (b) the relative position between the major Yb site and the geometric center of carbon cage (shallow blue point) in **2a**.

## 5. Crystal data of 2a

**Table S1.** Crystal data and structure refinement for **2a**

Identification code	<b>2a</b>
Empirical formula	C <sub>287</sub> H <sub>153</sub> CIN <sub>33</sub> Yb
Formula weight	4270.61
Temperature/K	293(2)
Crystal system	monoclinic
Space group	P2 <sub>1</sub> /n
a/Å	21.677
b/Å	30.619
c/Å	29.418
α/°	90
β/°	98.57
γ/°	90
Volume/Å <sup>3</sup>	19307.4
Z	4
ρ <sub>calc</sub> g/cm <sup>3</sup>	1.469
μ/mm <sup>-1</sup>	0.573
F(000)	8770.0
Crystal size/mm <sup>3</sup>	0.08 × 0.07 × 0.07
Radiation	synchrotron ( $\lambda = 0.710$ )
2θ range for data collection/°	1.93 to 38.668
Reflections collected	115764
Independent reflections	15764 [R <sub>int</sub> = 0.038, R <sub>sigma</sub> = 0.0922]
Data/restraints/parameters	15764/4173/4185
Goodness-of-fit on F <sup>2</sup>	0.964
Final R indexes [I>=2σ (I)]	R <sub>1</sub> = 0.0567, wR <sub>2</sub> = 0.1388
Final R indexes [all data]	R <sub>1</sub> = 0.1207, wR <sub>2</sub> = 0.1707
Largest diff. peak/hole / e Å <sup>-3</sup>	0.38/-0.30

**Table S2.** The comparison of these Di-EMFs with different carbon cage sizes.

Crystal of Di-EMFs	Encaged Yb disorders	Distance between main Yb and cage	Addition pattern
Yb@ $D_{3h}$ -C <sub>74</sub> derivative ( <b>2a</b> )	Yb1(0.37), Yb2(0.30), Yb2(0.26), Yb4(0.07)	Yb1-C1 (1.96 Å), Yb1-C2 (2.09 Å)	[6,6]-closed addition
Yb@C <sub>2v</sub> (3)-C <sub>80</sub> -Ad	Yb1(0.43), Yb2(0.18), Yb3(0.14), Yb4(0.14), Yb5(0.04), Yb6(0.04), Yb7(0.03)	Yb1-C1 (2.43 Å), Yb1-C2 (2.48 Å)	[5,6]-open addition
Yb@C <sub>2</sub> (13)-C <sub>84</sub> -Ad	Yb1(0.32), Yb2(0.29), Yb2(0.22), Yb4(0.09), Yb5(0.08)	Yb1-C1 (2.29 Å), Yb1-C2 (2.34 Å)	[5,6]-closed addition

## 6. Theoretical calculation of Yb@ $D_{3h}$ -C<sub>74</sub> and **2a**

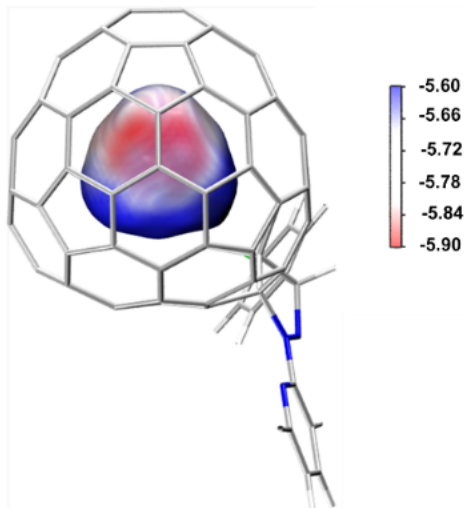


**Figure S4.** The electrostatic potential of the 2<sup>-</sup> charged outer cage of **2a**.

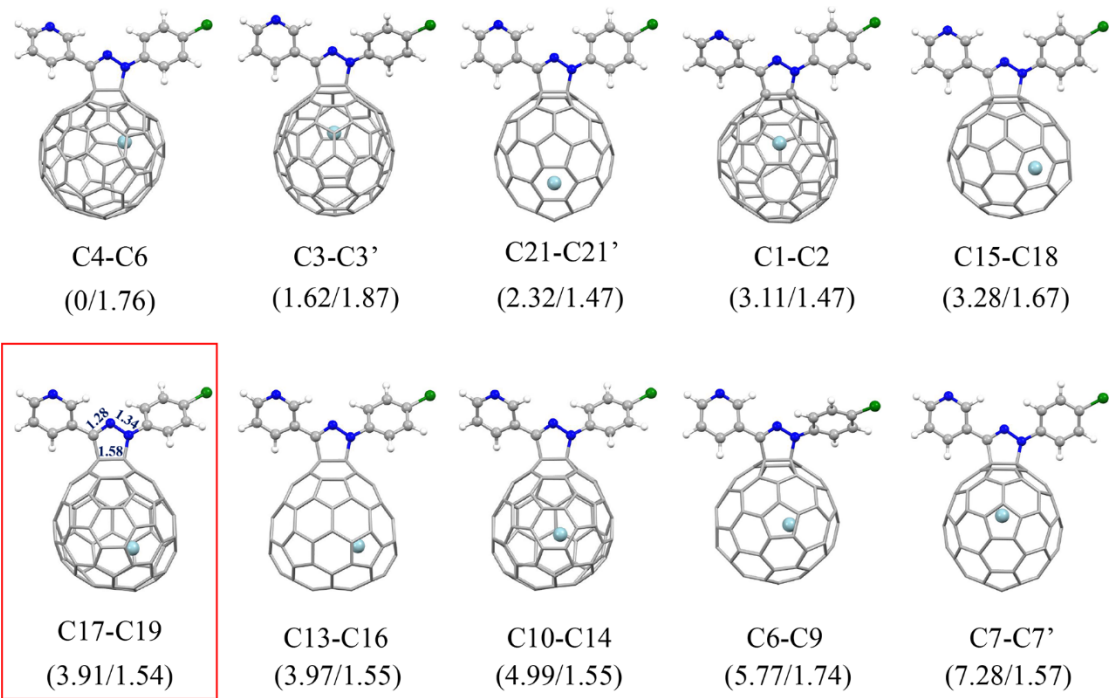


**Figure S5.** Optimized structures of ten low-energy  $\text{Yb}@D_{3h}\text{-C}_{74}$  adducts with relative energies (kcal/mol)/HOMO-LUMO gap energies (eV) in parenthesis. The selected distances are given in Å. C: gray, N: blue, H: white, Cl: green, Yb: light blue. The single crystal structure is highlighted in red box.

**Table S3** Relative energies(kcal/mol) and HOMO-LUMO gap energies(eV) of different Yb@ $D_{3h}$ -C<sub>74</sub>(C<sub>12</sub>N<sub>3</sub>H<sub>8</sub>Cl) adducts obtained at different levels of theory.

Addition	Bond type	PBE0		M06-2X	
		site	$\Delta E$	Gap	$\Delta E$
4-6	[5,6]		<b>0</b>	1.76	<b>0</b>
3-3'	[5,6]		1.62	1.87	0.53
21-21'	[5,6]		2.32	1.47	1.68
1-2	[5,6]		3.11	1.47	4.37
15-18	[5,6]		3.28	1.67	2.48
<b>17-19</b>	<b>[6,6]</b>		<b>3.91</b>	<b>1.54</b>	<b>3.82</b>
13-16	[6,6]		3.97	1.55	-
10-14	[6,6]		4.99	1.55	-
6-9	[5,6]		5.77	1.74	-
7-7'	[5,6]		7.28	1.57	-

## 7. Electrochemical data of Yb@ $D_{3h}$ -C<sub>74</sub> and 2a.

**Table S4.** Redox potentials (V vs. Fc<sup>+</sup>/Fc)<sup>[a]</sup> and electrochemical gaps( $\Delta E_{EC}$ ) of Yb@ $D_{3h}$ -C<sub>74</sub> and 2a.

Compound	<sup>ox</sup> $E_2$ (eV)	<sup>ox</sup> $E_1$ (eV)	<sup>red</sup> $E_1$ (eV)	<sup>red</sup> $E_2$ (eV)	<sup>red</sup> $E_3$ (eV)	<sup>red</sup> $E_2$ (eV)	HOMO/ LUMO	$\Delta E_{EC}$ (eV)	
Yb@ $D_{3h}$ -C <sub>74</sub>	-	+0.26	-0.81	-1.28	-	-	5.06/3.99	1.07	Ref. 15
<b>2a</b>	+0.62	+0.15	-0.78	-1.18	-1.89	-2.04	4.95/4.02	0.93	This work
Yb@C <sub>2v</sub> (3)-C <sub>80</sub>	+0.78	+0.34	-0.89	-1.27	-1.87	-2.13	5.14/3.91	1.23	Ref. 9
<b>2</b>	+0.66	+0.13	-0.81	-1.34	-1.76	-2.13	4.93/3.99	0.94	Ref. 9
Yb@C <sub>2</sub> (13)-C <sub>84</sub>	-	+0.45	-0.95	-1.16	-1.50	-1.76	5.25/3.85	1.40	Ref. 19
<b>2b</b>	+0.84	+0.34	-1.11	-1.44	-1.74	-2.19	5.14/3.69	1.45	Ref. 19

[a] DPV values on a Pt-working electrode in 1,2-dichlorobenzene; HOMO and LUMO values calculated according to the equation of  $E_{LUMO}=-e(E_{red}^{onset}+4.8\text{ V})$ ;  $E_{HOMO}=-e(E_{ox}^{onset}+4.8\text{ V})$ .

## Reference:

- [1] C. Adamo and V. Barone, *J. Chem. Phys.* 1999, **110**, 6158.
- [2] W. J. Hehre, R. Ditchfield and J. A. Pople, Self-Consistent Molecular Orbital Methods. XII. Further Extensions of Gaussian-Type Basis Sets for Use in Molecular Orbital Studies of Organic Molecules, *J. Chem. Phys.*, 1972, **56**, 2257-2261.
- [3] M. Dolg, H. Stoll and H. Preuss, Energy - adjusted ab initio pseudopotentials for the rare earth elements. *J. Chem. Phys.*, 1989, **90**, 1730–1734.
- [4] M. J. Frisch, G. W. Trucks, H. B. Schlegel, G. E. Scuseria, M. A. Robb, J. R. Cheeseman, G. Scalmani, V. Barone, G. A. Petersson, H. Nakatsuji, X. Li, M. Caricato, A. V. Marenich, J. Bloino, B. G. Janesko, R. Gomperts, B. Mennucci, H. P. Hratchian, J. V. Ortiz, A. F. Izmaylov, J. L. Sonnenberg, D. Williams-Young, F. Ding, F. Lipparini, F. Egidi, J. Goings, B. Peng, A. Petrone, T. Henderson, D. Ranasinghe, V. G. Zakrzewski, J. Gao, N. Rega, G. Zheng, W. Liang, M. Hada, M. Ehara, K. Toyota, R. Fukuda, J. Hasegawa, M. Ishida, T. Nakajima, Y. Honda, O. Kitao, H. Nakai, T. Vreven, K. Throssell, J. A. Montgomery, Jr., J. E. Peralta, F. Ogliaro, M. J. Bearpark, J. J. Heyd, E. N. Brothers, K. N. Kudin, V. N. Staroverov, T. A. Keith, R. Kobayashi, J. Normand, K. Raghavachari, A. P. Rendell, J. C. Burant, S. S. Iyengar, J. Tomasi, M. Cossi, J. M. Millam, M. Klene, C. Adamo, R. Cammi, J. W. Ochterski, R. L. Martin, K. Morokuma, O. Farkas, J. B. Foresman, and D. J. Fox, Gaussian 16, Revision C.01, Gaussian, Inc., Wallingford CT, 2019.
- [5] C. F. Macrae, P. R. Edgington, P. McCabe, E. Pidcock, G. P. Shields, R. Taylor, M. Towler, J. van de Streek, Mercury: Visualization and Analysis of Crystal Structures, *J. Appl. Crystallogr.*, 2006, **39**, 453-457.